

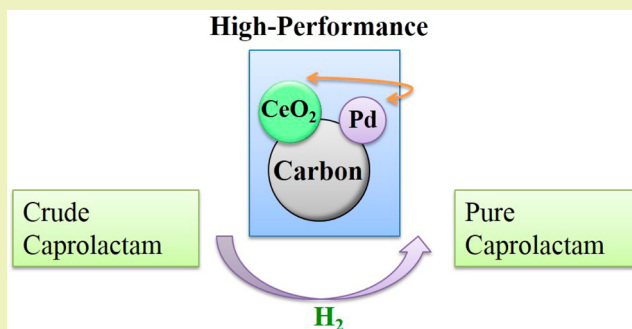
Ceria-Modified Palladium/Activated Carbon as a High-Performance Catalyst for Crude Caprolactam Hydrogenation Purification

Chunyan Tu and Shibiao Cheng*

State Key Laboratory of Catalytic Materials and Reaction Engineering, Research Institute of Petroleum Processing, China Petroleum & Chemical Corporation, Beijing 100083, China

ABSTRACT: A series of Pd/C catalysts modified with CeO₂ were characterized by X-ray diffraction (XRD), transmission electron microscopy–energy dispersive X-ray spectroscopy (TEM-EDX), temperature-programmed reduction (TPR), hydrogen chemisorption, and temperature-programmed desorption (TPD) measurements. The influence of CeO₂ additive on the physicochemical and catalytic properties of Pd/C catalyst was investigated. The addition of CeO₂ facilitated the reduction of PdO, while the presence of Pd shifted the reduction temperature of CeO₂ to lower values. Thus, a synergistic effect between Pd and CeO₂ was observed on these CeO₂-modified Pd/C catalysts. Both the dispersion of Pd and the hydrogen adsorption strength were significantly promoted by the addition of CeO₂. Moreover, Pd-CeO₂/C catalysts presented high catalytic performance for crude caprolactam (CPL) hydrogenation purification in comparison with Pd/C catalyst, which may be attributed to higher dispersion, stronger hydrogen adsorption strength, and better reduction behavior. The crude caprolactam was purified, and pure and high-quality ϵ -caprolactam was obtained. The 2% Pd–4% CeO₂/C catalyst, which exhibits especially high catalytic performance with CPL purity of 99.9955% and permanganate number of 24 000 s, is found to be more active than 5% Pd/C catalyst.

KEYWORDS: Palladium, Ceria, Activated carbon, Caprolactam, Hydrogenation, Purification, TPR, TPD



INTRODUCTION

The growing demand for clean and sustainable technology for producing bulk and fine chemicals is one of the driving forces in seeking environmentally benign processes. ϵ -Caprolactam is an intermediate for Nylon 6 fibers and resins, of which about 4 million tonnes are produced annually worldwide using methods that are not entirely environmentally sustainable.^{1,2}

In a widely used current ϵ -caprolactam production process, Beckmann rearrangement of cyclohexanone oxime into ϵ -Caprolactam has been carried out using corrosive oleum or sulfuric acid as a reaction promoter.³ Large quantities of ammonium sulfate are formed as a byproduct in this large-scale industrial process. Crude caprolactam obtained by Beckmann rearrangement is not sufficiently pure for polymer products. It is therefore purified by combined extraction, crystallization, distillation methods, and so on.^{4–8} In the DSM process,^{3,9} the crude caprolactam is first extracted with benzene and then reextracted with water. Before being distilled, the caprolactam extract is subjected to a number of physicochemical purifications, such as ion exchange treatment and hydrogenation with Raney nickel catalyst.³ However, the complicated purification process requires high energy and water consumption and produces large amounts of industrial liquid wastes. Moreover, Raney nickel catalyst has a short lifetime, environmental pollution caused by alkaline leaching during

their preparation, and low efficiency for the hydrogenation purification of crude caprolactam.^{10,11}

As the profitability of caprolactam production greatly depends on the byproducts and the complicated production processes, new processes have been sought by industry and academia for a long time.^{12–15} Sumitomo Chemical Co., Ltd., has commercialized the fluidized bed vapor-phase Beckmann rearrangement process, in which cyclohexanone oxime is converted to caprolactam on a high silica MFI zeolite catalyst with only water as a byproduct.¹⁴ The combined process of distillation, crystallization, and subsequent hydrogenation with palladium (Pd)-activated carbon catalyst has been proposed by Sumitomo Chemical Co., Ltd., for the purification of crude caprolactam. China Petrochemical Co., Ltd., focusing on the development of a sustainable route that is not energy-intensive and mitigates the production of waste, has developed the fixed-bed vapor-phase Beckmann rearrangement process which differs from the Sumitomo Chemical process. With regard to purification of crude caprolactam, a process in which crystallization is followed by hydrogenation is being developed.

The Pd/C catalyst is one of the most widely utilized catalysts in the process of catalytic hydrogenation for its higher catalytic activity and selectivity.^{16–19} For the Pd/C catalyst, Pd can

Received: August 1, 2013

Published: December 26, 2013

disperse on activated carbon support which has a broad specific surface area and a variety of functional groups. However, the limited availability and prohibitive cost of Pd catalyst have hampered their sustainable applications. Replacing or reducing the content of noble metals in industrial catalysts has become a major challenge in terms of catalyst applications.^{20,21} Therefore, the development of an environmentally benign catalyst that is more active and has a low content of noble metal is highly desirable and of great industrial significance. Great efforts have been made to optimize the preparation conditions and to understand the precursor-support interaction to improve the catalytic performance of Pd/C.^{22–29} But few studies on CeO₂ as a modifier of Pd/C catalyst have been reported. CeO₂ with a unique crystal structure is considered to be a material with a great capacity to release oxygen reversibly and undergo cycles of oxidation–reduction.^{29–31} CeO₂ can also affect the dispersion of the active phase and the heterogeneous catalytic reactions. It has been reported that the addition of ceria can generally improve the behavior of alumina based catalysts in olefin hydrogenation, CO low-temperature oxidation, and methanol decomposition.^{32–34}

In this study, the CeO₂-modified Pd/C catalyst is first used as a hydrogenation catalyst for hydrogenation purification of crude caprolactam, which is originally synthesized by fixed-bed vapor-phase Beckmann rearrangement of cyclohexanone oxime and then treated through a crystallization process. The purpose of this study is to investigate the physicochemical properties of the CeO₂-modified catalysts and clarify the effect of CeO₂ on the catalytic performance of Pd/C catalyst for crude caprolactam hydrogenation purification.

EXPERIMENTAL SECTION

Preparation of Catalysts. The support used in the preparation of all catalysts was activated carbon, with the following characteristics: coconut shell, BET specific surface area 1009 m²/g, pore volume 0.494 cm³/g. The activated carbon was previously treated with nitric acid. The resulting support was washed with distilled water several times and dried in air at 100 °C. The Pd/C catalysts with 2 or 5 wt % Pd were prepared by wet impregnation method with palladium nitrate as the precursor salt, using activated carbon granules (10 g) as the support. After impregnation, the catalysts were dried in an oven and followed by calcination. The CeO₂-modified Pd/C catalysts were prepared by coimpregnation method with the solutions containing the palladium nitrate and cerium nitrate salts. The procedure was the same as for the preparation of the Pd/C catalysts. The Pd content of CeO₂-modified Pd/C catalysts was about 2 wt %, and the CeO₂ content of those were 1–4 wt %.

Catalyst Characterization. X-ray diffraction (XRD) analysis was conducted on a D/MAX-III A X-ray diffractometer ((Rigaku Corporation, Japan) with filtered Cu K α radiation at a tube current of 35 mA and a voltage of 35 kV. The scanning range of 2 θ was 15–70°.

The morphology of the samples were observed by a Tecnai G² F20 field emission transmission electron microscope (FE-TEM) (FEI, Netherlands), and the chemical composition characteristics of the samples were studied by TEM equipped with X-ray energy dispersive spectroscopy (EDX).

The reducibility of catalysts was determined by temperature programmed reduction (TPR) experiments in an AutoChem II 2920 chemisorption analyzer (Micromeritics, USA). Prior to analysis, the sample (0.15 g) was flushed at 150 °C for 30 min with argon (30 mL/min) and then cooled to 50 °C. TPR profiles were registered by heating the samples to 750 °C, at 10 °C/min, in a H₂/Ar (10/90) mixture (30 mL/min).

Hydrogen chemisorption and temperature programmed desorption (TPD) were carried out in a AutoChem II 2920 chemisorption

analyzer (Micromeritics, USA), where Pd/C and Pd-CeO₂/C catalysts were pretreated at 150 °C for 30 min under Ar flow before the adsorption. The samples were reduced in a stream of pure hydrogen at room temperature to 200 °C, to protect the palladium from sintering. The reduced samples were swept with a flow of Ar for 30 min and cooled down to 50 °C. Hydrogen pulses from a H₂/Ar (10/90) mixture were injected into the Ar flow until saturation adsorption was reached. The samples were then thoroughly swept with Ar for 30 min and the TPD measurements were conducted in the Ar flow to 600 °C at the rate of 10 °C/min.

Catalytic Performance Test. High purity of industrial caprolactam is requested by users. The most important quality criteria are the parts per million amounts of impurities which can be oxidized with potassium permanganate, as well as the basic impurities which are present in free or volatile form.³ The permanganate number is considered to be one of the most important quality specifications of industrial caprolactam. Hydrogenation performance of the catalysts can be evaluated by the permanganate number of the reaction product, which is a measure of its oxidizability.⁵ A higher permanganate number indicates lower unsaturated impurities in a caprolactam aqueous solution.

The permanganate number of caprolactam can be measured by visual comparison with a standard solution, which is composed of 3 g Co(NO₃)₂·6H₂O and 0.012 g K₂Cr₂O₇ in 1 L of water.³ One milliliter of 0.01 mol/L potassium permanganate solution is added to 100 mL of 3 wt % aqueous caprolactam solution at 20 °C. The time (s) taken for the color to change to that of the standard solution is referred to as the permanganate number.

The hydrogenation purification of crude caprolactam with CPL purity of 99.9887% and a permanganate number of 200 s was used as an objective reaction. The crude caprolactam, synthesized by vapor-phase Beckmann rearrangement of cyclohexanone oxime and then treated through distillation and crystallization steps, was provided by the Research Institute of Petroleum Processing of China. All the reactions were carried out in a stainless steel agitated autoclave (500 mL) equipped with an external manometer and a mass flow controller. The washed crystalline caprolactam (75 g) was dissolved in water (175 g) and the solution was charged into the autoclave. Then, a catalyst (40–60 mesh, 0.25 g) was added into the aqueous solution. The autoclave was pressurized to 0.77 MPa with hydrogen and heated to 90 °C, together with a hydrogen gas flow at a flow rate of 600 mL/min. In this case, the catalyst was reduced in situ. Hereafter, the hydrogenation reaction was performed at 90 °C, 0.77 MPa, 320 r/min of stirring speed, and a constant H₂ flow rate of 600 mL/min for 1 h. The catalytic performance was illustrated by the CPL purity and the permanganate number of the reaction product. The CPL purity of the reaction product was analyzed with a gas chromatography (Agilent 7890, USA) equipped with a flame ionization detector (FID) and a PEG20000 column (60 m × 0.32 mm × 0.5 μ m).

RESULTS AND DISCUSSION

X-ray Diffraction. Figure 1 shows the XRD patterns of activated carbon, CeO₂/C, Pd/C, and Pd-CeO₂/C. As can be

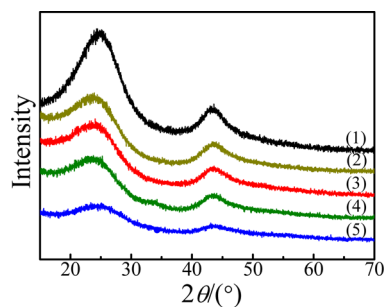


Figure 1. XRD patterns of samples: (1) C (support); (2) 1% CeO₂/C; (3) 2% Pd/C; (4) 2% Pd–1% CeO₂/C; (5) 2% Pd–4% CeO₂/C.

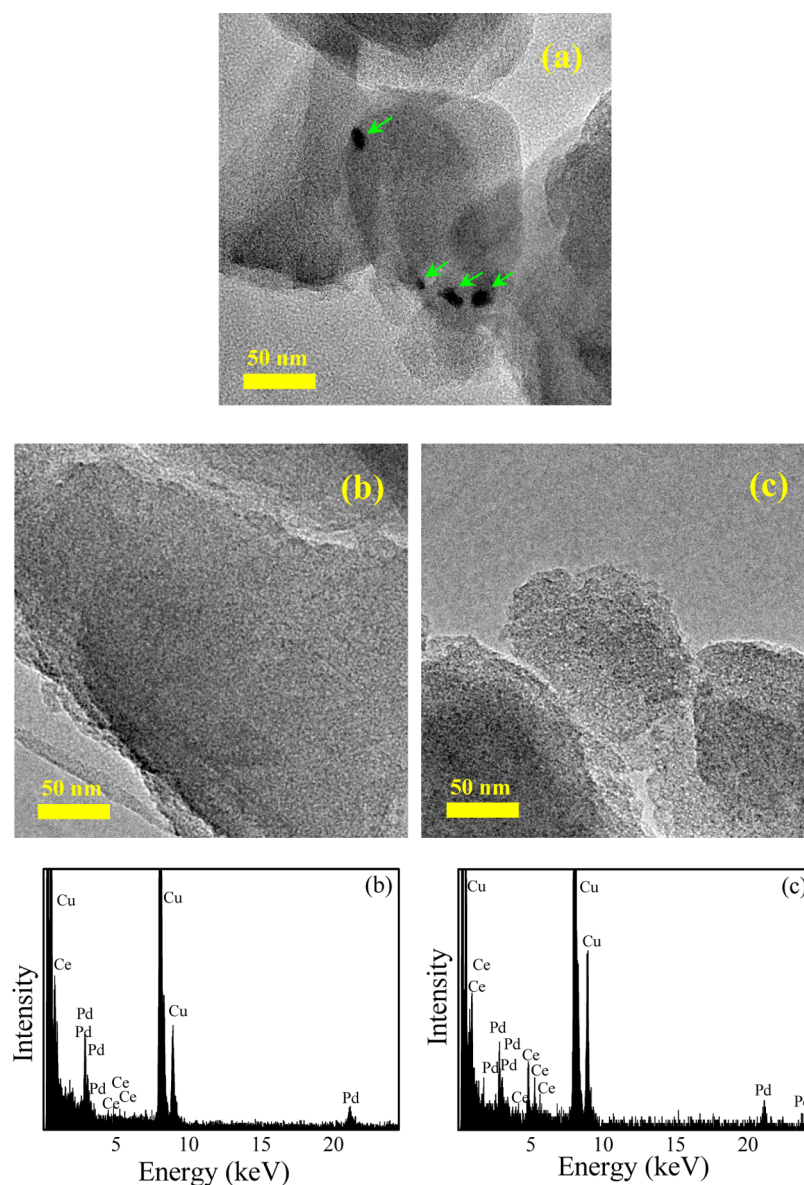


Figure 2. TEM-EDX images of the 2% Pd- $x\%$ CeO₂/C samples with different CeO₂ loading: (a) 0; (b) 1%; (c) 4%.

seen, all these patterns have similar features in their shapes. The diffraction peaks at 24.0° and 43.5° are ascribed to activated carbon. In the case of 2% Pd-4% CeO₂/C, the peaks due to activated carbon become far weaker compared with other samples. No diffraction peaks of Pd metal, PdO, and CeO₂ are observed, which is evidence of nanoscale particle size.²⁸ The inclusion of Pd and Ce components in the samples seems to result in the weaker peaks of activated carbon. It is well accepted that the X-ray patterns of metal and metal oxide species are not observed because metals and metal oxides are highly dispersed on the support.²⁹ Hence, it can be concluded that Pd disperses well from Pd/C and Pd-CeO₂/C catalysts.

TEM-EDX Characterization. Figure 2 shows the TEM images of the Pd-CeO₂/C samples with different CeO₂ loading. It can be seen that all these samples exhibit good dispersion states, which is in agreement with the results from the XRD measurements. In the 2% Pd/C sample, a few aggregated Pd particles are observed. However, no aggregation is found for the Pd-CeO₂/C samples. EDX analyses of the whole section under observation (TEM image of Figures 2a or

b) indicate that both Pd and Ce components are present in the 2% Pd-1% CeO₂/C and 2% Pd-4% CeO₂/C samples. It is noted that the inclusion of CeO₂ prevents the aggregation of Pd fine particles, thus making surface Pd sites more available. As a result, the Pd-CeO₂/C catalysts exhibit a better dispersion than the Pd/C catalyst. Yamashita et al.³⁵ and Resasco et al.^{36,37} also demonstrated that CeO₂ could inhibit the aggregation of noble metal particles, which was attributed to the strong interaction between CeO₂ and noble metal.

Temperature Programmed Reduction. The H₂-TPR profiles of PdO and CeO₂ are displayed in Figure 3. A sharp, negative peak at 67 °C is observed in the TPR profile of pure palladium oxide, indicating that pure palladium oxide is reduced below 50 °C. Hydrogen desorption with a maximum at a temperature 50–100 °C has been reported in the literature^{38–40} and is ascribed to the desorption of weakly adsorbed hydrogen from the palladium surface and to the decomposition of palladium hydride formed at room temperature. In hydrogen atmosphere, PdO gets reduced easily at ambient temperature to Pd metal, and further interacts with hydrogen, forming PdH_x,

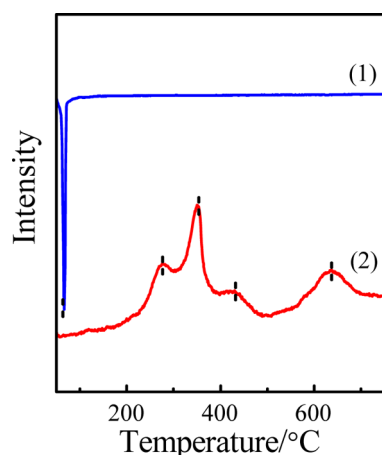


Figure 3. H₂-TPR profiles of samples: (1) PdO; (2) CeO₂.

which appears to have occurred during the passage of reducing gas prior to the start of the temperature program.^{40,41} Note that cerium oxide is reduced at a higher temperature, with maximum peaks at 275, 351, 432, and 640 °C. According to Shyu et al.⁴² and de Leitenburg et al.,⁴³ the reduction of bulk ceria is stepwise by hydrogen. Specifically, these reduction peaks are probably associated with reduction of the surface oxygen of CeO₂, formation of nonstoichiometric Ce oxides (CeO_x with *x* ranging from 1.9 to 1.7, or β phase), and the total reduction of ceria to Ce₂O₃.⁴²

Figure 4 presents the H₂-TPR profiles of activated carbon, CeO₂/C, Pd/C, and Pd–CeO₂/C catalysts. Activated carbon

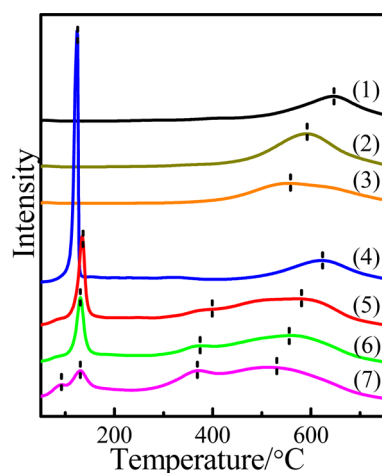


Figure 4. H₂-TPR profiles of samples: (1) C (support); (2) 1% CeO₂/C; (3) 4% CeO₂/C; (4) 2% Pd/C; (5) 2% Pd–1% CeO₂/C; (6) 2% Pd–2% CeO₂/C; (7) 2% Pd–4% CeO₂/C.

shows a maximum peak around 644 °C, which can be attributed to the reduction of the surface groups of activated carbon. For the 1% CeO₂/C catalyst, a high hydrogen consumption peak at 591 °C is observed. Similarly, the profile of the 4% CeO₂/C catalyst displays one hydrogen uptake, beginning at 400 °C with a maximum peak at 552 °C. It should be noted that the hydrogen consumption due to activated carbon shifts to a lower temperature with CeO₂ loading increase. The Pd/C catalyst shows two hydrogen uptakes, one at 124 °C assigned to PdO reduction and the other at 621 °C ascribed to activated carbon. In this case, the shift to a lower temperature of the hydrogen

consumption of activated carbon is due to the gasification of the support promoted by metallic palladium. A similar result is also reported by Noronha et al.³⁸

The TPR profiles of Pd–CeO₂/C catalysts are different when compared to the Pd/C catalyst. The 2% Pd–1% CeO₂/C and 2% Pd–2% CeO₂/C catalysts exhibit reduction peaks of PdO at 135 °C for 2% Pd–1% CeO₂/C and 131 °C for 2% Pd–2% CeO₂/C, respectively. The 2% Pd–4% CeO₂/C catalyst displays two hydrogen uptakes at 93 and 130 °C, attributable to PdO reduction. It also can be seen that the peak intensity is related to ceria loading. According to Monteiro et al.,³⁴ the splitting into two peaks and the peak intensity change suggests different interaction levels between PdO species and ceria. It can be assumed that palladium oxide particles are deposited over activated carbon, ceria, and the ceria-activated carbon interface during the preparation of Pd–CeO₂/C catalysts. For the Pd/C catalyst, palladium oxide particles are deposited on the surface of activated carbon. Therefore, the strong interaction between Pd–Ce shifts the PdO reduction peak down to a lower temperature or even to room temperature, while small PdO particles that have strongly interacted with the support are less likely to be reduced. For Pd–CeO₂/C catalysts, the hydrogen uptake around 130 °C is assigned to the reduction of PdO deposited on activated carbon. The difficulty of reduction is ascribed to the extensive spreading of small particles on the support because of the dilution effect of ceria. In the case of the 2% Pd–4% CeO₂/C catalyst, the minor peak at 93 °C is attributed to the reduction of PdO contacted with CeO₂. Compared with the 2% Pd/C catalyst, the peak due to the PdO deposited on the support becomes weaker with the increase of CeO₂ loading, while the peak assigned to PdO contacted with CeO₂ becomes stronger. More importantly, due to the strong Pd–Ce interaction, amounts of PdO particles are likely to be reduced below 50 °C or even at room temperature, as shown by lower hydrogen consumption between 50 and 200 °C in Pd–CeO₂/C catalysts, less than that necessary to reduce the PdO in the Pd/C catalyst. Thus the reduction of palladium oxide is promoted by the addition of ceria.

From the profile of the 2% Pd–1% CeO₂/C catalyst, the reduction of ceria is clearly observed, beginning at 279 °C and with a peak at 401 °C. The hydrogen consumption peak assigned to the support seems to partially overlap with the reduction peaks of ceria. The 2% Pd–2% CeO₂/C and 2% Pd–4% CeO₂/C catalysts distinctly present one main hydrogen uptake due to CeO₂ reduction, 375 °C for 2% Pd–2% CeO₂/C and 371 °C for 2% Pd–4% CeO₂/C. It also can be seen that the reduction peak intensity increases with ceria loading increase. Numerous studies have reported that the reduction temperature of metal oxide by H₂ can be lowered by the addition of palladium.⁴⁴ The effect of Pd can be attributed to hydrogen spillover from Pd particles, leading to activated hydrogen atoms which can increase the reduction rate of metal oxide.^{44,45} Thus ceria particles tend to be reduced more easily in the presence of palladium. This behavior is more evident in higher ceria content catalysts.

The reduction behavior of the catalysts is affected by the Pd–Ce interaction. The presence of ceria lowers the reduction temperature of palladium oxide, while palladium similarly facilitates the reduction of ceria species. Therefore, these results indicate that a synergistic effect between palladium and ceria exists in Pd–CeO₂ catalysts. A similar synergistic effect between

Pd and CeO₂ or CeO₂-TiO₂ is also reported by Zhu⁴⁶ and Jin.⁴⁷

Hydrogen Chemisorption. Table 1 shows the hydrogen chemisorption results of various samples. It can be seen that

Table 1. Chemisorption Results of Samples

sample	volume of chemisorbed H ₂ (μL H ₂ /mg sample)	amount of chemisorbed H ₂ (μmol H ₂ /mg Pd)	H/Pd ratio
C (support)	0		
2% CeO ₂ /C	0		
2% Pd/C	0.97	2.18	0.46
2% Pd-1% CeO ₂ /C	1.03	2.29	0.49
2% Pd-2% CeO ₂ /C	1.05	2.35	0.50
2% Pd-4% CeO ₂ /C	0.97	2.17	0.46

activated carbon support and CeO₂/C cannot chemisorb hydrogen. The hydrogen adsorption capacity of the samples containing 1 and 2 wt % CeO₂ is slightly higher than that of the Pd/C sample. But the differences in the values of "H/Pd" for each sample shown in Table 1 are rather small. Although H₂ adsorption for measuring metal dispersion of noble metal catalyst has been well-known, the hydrogen adsorption method for Pd dispersion measurement that is based on direct adsorption has less applicability.⁴⁸ Because they require the complete removal of hydrogen used for reduction from the metal surface. As reported in the literature,^{34,49} H₂ spilling effect can increase H₂ uptake, while dilution by inactive ceria on Pd can decrease the total number Pd active sites available for H₂ adsorption. An intermetallic complex is formed, due to the strong interaction of Pd-Ce, affecting hydrogen chemisorption.³⁴ On the basis of these studies, the three possible cases might result in the small differences in hydrogen adsorption capacity for Pd/C and Pd-CeO₂/C catalysts.

Hydrogen Temperature-Programmed Desorption.

Figure 5 presents the H₂-TPD profiles for activated carbon,

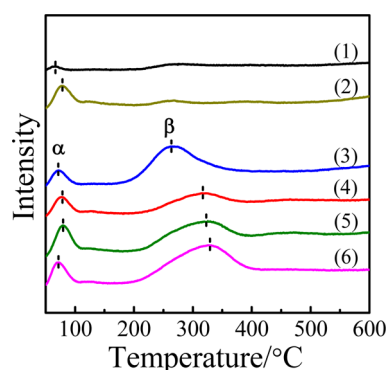


Figure 5. H₂-TPD profiles of samples: (1) C (support); (2) 2% CeO₂/C; (3) 2% Pd/C; (4) 2% Pd-1% CeO₂/C; (5) 2% Pd-2% CeO₂/C; (6) 2% Pd-4% CeO₂/C.

CeO₂/C, Pd/C, and Pd-CeO₂/C catalysts with various CeO₂ loadings. Activated carbon shows a weak desorption peak around 66 °C. In the case of 2% CeO₂/C, a higher hydrogen desorption at 78 °C is observed, suggesting that ceria favors the adsorption of hydrogen. The H₂-TPD profile of the 2% Pd/C catalyst shows two desorption peaks: one at 71 °C and the other at 263 °C. This indicates that two different adsorbed states of hydrogen exist on the catalyst. The more weakly bound state has the lower activation energy for desorption and

will therefore undergo desorption at a lower temperature. According to Webb,⁵⁰ the low temperature peak (peak α) corresponds to the weak adsorption of molecular hydrogen and relates to desorption from the support; whereas the high temperature peak (peak β) corresponds to dissociatively adsorbed hydrogen on the catalyst.

Interestingly, with the addition of 1% ceria, peak α shows little change, while peak β significantly moves to a higher temperature (316 °C) and its peak intensity decreases. This indicates that the hydrogen adsorption properties (based on peak β) of Pd/C catalyst are likely to be related to the interaction between Pd and CeO₂. There is some consensus in the literature that the decrease of hydrogen chemisorption capacity can be mainly explained by a geometric effect.³⁴ Specifically, dilution by inactive ceria on Pd decreases the total number Pd active sites available for H₂ adsorption. Further, it should be noted that the hydrogen adsorption strength of Pd/C catalyst is strongly enhanced by the addition of CeO₂. The asymmetric peak β in the TPD profile of 2%Pd-1%CeO₂/C probably corresponds to the desorption peak of hydrogen dissociatively adsorbed on the palladium particles, partially overlapping with the evolution peak of another kind of hydrogen from the catalyst. Amorim et al.⁵¹ once demonstrated that hydrogen spillover could be generated at room temperature. Removal of spillover hydrogen requires temperatures in excess of 230 °C, regardless of the nature of the metal or support.⁵¹⁻⁵⁴ Ouchaib et al.⁵⁵ attributed the hydrogen desorption peak from charcoal supported Pd at 400 °C to spillover hydrogen. As reported in the literature,⁴⁹ in a hydrogen spillover system, oxygen groups doping in carbon materials leads to stronger adsorption for the spillover hydrogen, in the presence of palladium. On the basis of these studies, the temperature required for desorption of spillover hydrogen is higher than that required for desorption of chemisorbed hydrogen from metallic palladium. It is likely that molecular hydrogen is dissociated on palladium particles, and the resulting atomic hydrogen can then migrate to adjacent ceria. Thus, the overlapping peak β in the TPD profile corresponds to hydrogen chemisorbed on Pd and spillover hydrogen on adjacent ceria.

With respect to the TPD behaviors of Pd-CeO₂/C catalysts with various CeO₂ loadings, as shown in Figure 5, further increase in ceria loading results in an obvious increase in both the peak intensity and the peak temperature of peak β , indicating that more hydrogen atoms have transferred to adjacent ceria allowing more hydrogen to chemisorb on the palladium. According to Wang et al.,⁴⁹ an intimate contact between Pd and CeO₂ facilitates the spillover and thus results in enhancement in hydrogen adsorption capacity. Therefore, it can be concluded that the hydrogen adsorption strength of Pd/C catalyst is distinctly enhanced with the increase of CeO₂ loading and the dissociative adsorption capacity of hydrogen is affected by both a geometric effect and hydrogen spillover to adjacent ceria.

Catalytic Performance in Hydrogenation Purification of Crude Caprolactam. The reaction results for Pd/C and Pd-CeO₂/C catalysts in hydrogenation purification of crude caprolactam are shown in Table 2. It is known that the hydrogenation effect of the catalysts is mainly presented by the permanganate number of the reaction product. It is seen that C (support) has no physical adsorption to the impurities of crude caprolactam and CeO₂/C almost has no effect on hydrogenation purification. However, both the commercial and

Table 2. Comparison of the Catalytic Performance of the Samples^a

sample	reaction product	
	CPL purity, %	permanganate number/s
C (support)	99.9901	248
1% CeO ₂ /C	99.9903	263
2% Pd/C (commercial)	99.9943	7500
2% Pd/C (homemade)	99.9962	9780
2% Pd–1% CeO ₂ /C	99.9962	13440
2% Pd–2% CeO ₂ /C	99.9963	19800
2% Pd–4% CeO ₂ /C	99.9955	24000
5% Pd/C	99.9960	16200

^aThe crude caprolactam with CPL purity of 99.9887%, and a permanganate number of 200 s was used as the starting material for the catalytic tests.

homemade 2% Pd/C catalyst (commercial 2%Pd/C supplied by the Northwest Institute for Nonferrous Metal Research of China) show a good hydrogenation effect with permanganate numbers of 7500 and 9780 s, respectively. The catalytic performance of Pd–CeO₂/C catalysts for the purification of crude caprolactam is better than that of Pd/C catalyst and is greatly improved with the increase of CeO₂ loading. The permanganate number of the reaction product increases distinctly, along with CPL purity of greater than 99.995%. The crude caprolactam is purified, and pure and high-quality ϵ -caprolactam is obtained. The 2% Pd–4% CeO₂/C catalyst, the CPL purity and permanganate number of which reached up to 99.9955% and 24 000 s, is found to be more active than 5% Pd/C catalyst. Therefore, compared with high loading Pd/C, ceria-doped Pd/C with lower Pd loading can exhibit equivalent or better catalytic performance in hydrogenation purification of crude caprolactam.

The catalytic performance of the Pd/C catalyst for the purification of crude caprolactam is enhanced with the addition of ceria, probably attributable to the interaction between Pd and CeO₂. As seen before, the addition of ceria facilitates the dispersion of Pd. Hydrogen chemisorption is inhibited by the Pd–Ce interaction, but the reaction activity itself is better. This may be explained by the occurrence of new active sites, specifically of spillover hydrogen, which increase the adsorption strength of hydrogen favoring hydrogenation.

As the ceria loading increases further, the catalytic performance of Pd–CeO₂/C catalysts is greatly improved. The strong interaction between Pd and CeO₂ greatly enhances the hydrogen adsorption strength and, thus, accelerates the reaction rate. Furthermore, the presence of ceria lowers the reduction temperature of the palladium oxide. In this case, more PdO could be reduced to Pd and many more new active sites could form at the interface of Pd–CeO₂. Therefore, the catalytic performance could be significantly enhanced by the greatly increasing active center.

CONCLUSIONS

The physicochemical properties of Pd/C and CeO₂-modified Pd/C catalysts have been investigated. The influence of CeO₂ on the catalytic performance of Pd/C catalyst for crude caprolactam hydrogenation purification is probably attributable to the interaction between Pd and CeO₂. The presence of CeO₂ lowers the reduction temperature of PdO, while Pd similarly facilitates the reduction of ceria species. There is a synergistic effect between Pd and CeO₂. The addition of CeO₂

could significantly promote the dispersion of Pd and the hydrogen adsorption strength of the Pd/C catalyst. Moreover, Pd–CeO₂/C catalysts present high catalytic performance for crude caprolactam hydrogenation purification in comparison with Pd/C catalysts, which may be attributed to higher dispersion, stronger hydrogen adsorption strength, and better reduction behavior. The crude caprolactam is purified, and pure and high-quality ϵ -caprolactam is obtained. The 2% Pd–4% CeO₂/C catalyst, which especially exhibits high catalytic performance with CPL purity of 99.9955% and a permanganate number of 24 000 s, is found to be more active than 5% Pd/C catalyst.

AUTHOR INFORMATION

Corresponding Author

*E-mail: sbcheng.ripp@sinopec.com.

Notes

The authors declare no competing financial interest.

ACKNOWLEDGMENTS

Financial support from the National Key Basic Research and Development Program (973 program, No. 2012 CB224804) is gratefully acknowledged.

REFERENCES

- (1) Mokaya, R.; Poliakov, M. Chemistry: A cleaner way to nylon? *Nature* **2005**, *437*, 1243–1244.
- (2) Tang, B.; Lin, Y.; Yu, P.; Luo, Y. Study of aniline/ ϵ -caprolactam mixture adsorption from aqueous solution onto granular activated carbon: Kinetics and equilibrium. *Chem. Eng. J.* **2012**, *187*, 69–78.
- (3) Ritz, J.; Fuchs, H.; Kieczka, H.; Moran, W. C. *Caprolactam*; Wiley-VCH: Weinheim, 2012.
- (4) Synowiec, J.; Synowiec, P. Industrial purification of caprolactam by means of crystallization from aqueous solution. *Cryst. Res. Technol.* **1983**, *18*, 951–957.
- (5) Jodra, L. G.; Romero, A.; Garcia-Ochoa, F.; Aracil, J. Impurity content and quality definition of commercial ϵ -caprolactam. *Ind. Eng. Chem. Product Res. Dev.* **1981**, *20*, 562–566.
- (6) Tan, K.; Hironaka, T.; Nakamura, M. *Method for producing high-purity caprolactam*. US Patent 4,900,821, Feb 13, 1990.
- (7) Jansens, P. J.; Langen, Y. H. M.; van den Berg, E. P. G.; Geertman, R. M. Morphology of ϵ -caprolactam crystals dependent on the crystallization conditions. *J. Cryst. Growth* **1995**, *155*, 126–134.
- (8) Diepen, P. J.; Bruinsma, O. S. L.; Rosmalen, G. M. V. Melt crystallization by controlled evaporative cooling. The caprolactam–water system in batch operation. *Chem. Eng. Sci.* **2000**, *55*, 3575–3584.
- (9) Guit, R.; Philippus, M.; Frentzen, Y. *Recovery of epsilon-caprolactam from aqueous mixtures*. WO Patent 1,997,030,028, Aug 21, 1997.
- (10) Ge, S.; Wu, Z.; Zhang, M.; Li, W.; Tao, K. Sulfolene Hydrogenation over an Amorphous Ni–B Alloy Catalyst on MgO. *Ind. Eng. Chem. Res.* **2006**, *45*, 2229–2234.
- (11) Liu, Y.-C.; Chen, Y.-W. Hydrogenation of p-Chloronitrobenzene on Lanthanum-Promoted NiB Nanometal Catalysts. *Ind. Eng. Chem. Res.* **2006**, *45*, 2973–2980.
- (12) Buntara, T.; Noel, S.; Phua, P. H.; Melián-Cabrera, I.; de Vries, J. G.; Heeres, H. J. Caprolactam from Renewable Resources: Catalytic Conversion of 5 - Hydroxymethylfurfural into Caprolactone. *Angew. Chem., Int. Ed.* **2011**, *50*, 7083–7087.
- (13) Ichihashi, H.; Ishida, M.; Shiga, A.; Kitamura, M.; Suzuki, T.; Suenobu, K.; Sugita, K. The Catalysis of Vapor-Phase Beckmann Rearrangement for the Production of ϵ -Caprolactam. *Catal. Surveys Asia* **2003**, *7*, 261–270.
- (14) Izumi, Y.; Ichihashi, H.; Shimazu, Y.; Kitamura, M.; Sato, H. Development and industrialization of the vapor-phase Beckmann rearrangement process. *Bull. Chem. Soc. Jpn.* **2007**, *80*, 1280–1287.

- (15) Komatsu, T.; Maeda, T.; Yashima, T. Kinetic study on the effect of solvent in 'vapor-phase' Beckmann rearrangement of cyclohexanone oxime on silicalite-1. *Microporous Mesoporous Mater.* **2000**, *35*, 173–180.
- (16) Auer, E.; Freund, A.; Pietsch, J.; Tacke, T. Carbons as supports for industrial precious metal catalysts. *Appl. Catal. A: Gen.* **1998**, *173*, 259–271.
- (17) Hattori, K.; Sajiki, H.; Hirota, K. Chemoselective control of hydrogenation among aromatic carbonyl and benzyl alcohol derivatives using Pd/C(en) catalyst. *Tetrahedron* **2001**, *57*, 4817–4824.
- (18) Bulushev, D. A.; Ross, J. R. H. Vapour phase hydrogenation of olefins by formic acid over a Pd/C catalyst. *Catal. Today* **2011**, *163*, 42–46.
- (19) Neri, G.; Musolino, M. G.; Milone, C.; Visco, A. M.; Di Mario, A. Mechanism of 2,4-dinitrotoluene hydrogenation over Pd/C. *J. Mol. Catal. A: Chem.* **1995**, *95*, 235–241.
- (20) Nørskov, J. K.; Bligaard, T.; Rossmeisl, J.; Christensen, C. H. Towards the computational design of solid catalysts. *Nat. Chem.* **2009**, *1*, 37–46.
- (21) Juan, J. B.-S.; Raghunath, V. C.; Bala, S. Design of Heterogeneous Catalysts for Fuels and Chemicals Processing: An Overview. *Novel Materials for Catalysis and Fuels Processing*; American Chemical Society, 2013; Vol. 1132, pp 3–68.
- (22) Li, J. Y.; Ma, L.; Li, X. N.; Lu, C. S.; Liu, H. Z. Effect of nitric acid, pretreatment on the properties of activated carbon and supported palladium catalysts. *Ind. Eng. Chem. Res.* **2005**, *44*, 5478–5482.
- (23) Gurrath, M.; Kuretzky, T.; Boehm, H. P.; Okhlopko, L. B.; Lisitsyn, A. S.; Likhobolov, V. A. Palladium catalysts on activated carbon supports - Influence of reduction temperature, origin of the support and pretreatments of the carbon surface. *Carbon* **2000**, *38*, 1241–1255.
- (24) Suh, D. J.; Park, T. J.; Ihm, S. K. Effect of surface oxygen groups of carbon supported on the characteristics of Pd/C catalysts. *Carbon* **1993**, *31*, 427–435.
- (25) Ryndin, Y. A.; Stenin, M. V.; Boronin, A. I.; Bukhtiyarov, V. I.; Zaikovskii, V. I. Effect of Pd/C dispersion on its catalytic properties in acetylene and vinylacetylene hydrogenation. *Appl. Catal.* **1989**, *54*, 277–288.
- (26) Watanabe, S.; Arunajatesan, V. Influence of acid modification on selective phenol hydrogenation over Pd/Activated carbon catalysts. *Top. Catal.* **2010**, *53*, 1150–1152.
- (27) Cabiac, A.; Cacciaguerra, T.; Trens, P.; Durand, R.; Delahay, G.; Medevielle, A.; Plée, D.; Coq, B. Influence of textural properties of activated carbons on Pd/carbon catalysts synthesis for cinnamaldehyde hydrogenation. *Appl. Catal. A: Gen.* **2008**, *340*, 229–235.
- (28) Cabiac, A.; Delahay, G.; Durand, R.; Trens, P.; Coq, B.; Plee, D. Controlled preparation of Pd/AC catalysts for hydrogenation reactions. *Carbon* **2007**, *45*, 3–10.
- (29) Hosokawa, S.; Taniguchi, M.; Utani, K.; Kanai, H.; Imamura, S. Affinity order among noble metals and CeO₂. *Appl. Catal. A: Gen.* **2005**, *289*, 115–120.
- (30) Colussi, S.; de Leitenburg, C.; Dolcetti, G.; Trovarelli, A. The role of rare earth oxides as promoters and stabilizers in combustion catalysts. *J. Alloys Compd.* **2004**, *374*, 387–392.
- (31) Soria, J.; Conesa, J. C.; Martínez-Arias, A. Characterization of surface defects in CeO₂ modified by incorporation of precious metals from chloride salts precursors: an EPR study using oxygen as probe molecule. *Colloids and Surfaces A: Physicochem. Eng. Aspects* **1999**, *158*, 67–74.
- (32) Lu, X.; Luo, L. T.; Chen, X. S. Influence of Pd-Ce interaction and chlorine ion on hydrodesulfurization reaction: The activity and sulfur tolerance of the Pd–CeO₂/Al₂O₃ catalyst. *React. Kinet. Catal. Lett.* **2008**, *94*, 35–46.
- (33) Monteiro, R. S.; Dieguez, L. C.; Schmal, M. The role of Pd precursors in the oxidation of carbon monoxide over Pd/Al₂O₃ and Pd/CeO₂/Al₂O₃ catalysts. *Catal. Today* **2001**, *65*, 77–89.
- (34) Monteiro, R. D. S.; Noronha, F. B.; Dieguez, L. C.; Schmal, M. Characterization of Pd-CeO₂ interaction on alumina support and hydrogenation of 1,3-butadiene. *Appl. Catal. A: Gen.* **1995**, *131*, 89–106.
- (35) Fuku, K.; Goto, M.; Sakano, T.; Kamegawa, T.; Mori, K.; Yamashita, H. Efficient degradation of CO and acetaldehyde using nano-sized Pt catalysts supported on CeO₂ and CeO₂/ZSM-5 composite. *Catal. Today* **2013**, *201*, 57–61.
- (36) Stagg-Williams, S. M.; Noronha, F. B.; Fendley, G.; Resasco, D. E. CO₂ Reforming of CH₄ over Pt/ZrO₂ Catalysts Promoted with La and Ce Oxides. *J. Catal.* **2000**, *194*, 240–249.
- (37) Noronha, F. B.; Fendley, E. C.; Soares, R. R.; Alvarez, W. E.; Resasco, D. E. Correlation between catalytic activity and support reducibility in the CO₂ reforming of methane over Pt/Ce_xZr_{1-x} O₂ catalysts. *Chem. Eng. J.* **2001**, *82*, 21–31.
- (38) Noronha, F. B.; Schmal, M.; Nicot, C.; Moraweck, B.; Frety, R. Characterization of graphite-supported palladium-cobalt catalysts by temperature-programmed reduction and magnetic measurements. *J. Catal.* **1997**, *168*, 42–50.
- (39) Chen, L. F.; Wang, J. A.; Valenzuela, M. A.; Bokhimi, X.; Acosta, D. R.; Novaro, O. Hydrogen spillover and structural defects in a PdO/zirconia nanophase synthesized through a surfactant-templated route. *J. Alloys Compd.* **2006**, *417*, 220–223.
- (40) Sangeetha, P.; Shanthi, K.; Rao, K. S. R.; Viswanathan, B.; Selvam, P. Hydrogenation of nitrobenzene over palladium-supported catalysts—Effect of support. *Appl. Catal. A: Gen.* **2009**, *353*, 160–165.
- (41) Padmasri, A.; Venugopal, A.; Krishnamurthy, J.; Rama Rao, K.; Kanta Rao, P. Novel calcined Mg-Cr hydrotalcite supported Pd catalysts for the hydrogenolysis of CCl₂F₂. *J. Mol. Catal. A: Chem.* **2002**, *181*, 73–80.
- (42) Shyu, J.; Weber, W.; Gandhi, H. Surface characterization of alumina-supported ceria. *J. Phys. Chem.* **1988**, *92*, 4964–4970.
- (43) de Leitenburg, C.; Trovarelli, A.; Llorca, J.; Cavani, F.; Bini, G. The effect of doping CeO₂ with zirconium in the oxidation of isobutane. *Appl. Catal. A: Gen.* **1996**, *139*, 161–173.
- (44) Conner, W. C., Jr; Falconer, J. L. Spillover in heterogeneous catalysis. *Chem. Rev.* **1995**, *95*, 759–788.
- (45) Luo, M. F.; Hou, Z. Y.; Yuan, X. X.; Zheng, X. M. Characterization study of CeO₂ supported Pd catalyst for low-temperature carbon monoxide oxidation. *Catal. Lett.* **1998**, *50*, 205–209.
- (46) Zhu, H. Q.; Qin, Z. F.; Shan, W. J.; Shen, W. J.; Wang, J. G. CO oxidation at low temperature over Pd supported on CeO₂-TiO₂ composite oxide. *Catal. Today* **2007**, *126*, 382–386.
- (47) Jin, M.; Park, J.-N.; Shon, J. K.; Kim, J. H.; Li, Z.; Park, Y.-K.; Kim, J. M. Low temperature CO oxidation over Pd catalysts supported on highly ordered mesoporous metal oxides. *Catal. Today* **2012**, *185*, 183–190.
- (48) Prelazzi, G.; Cerboni, M.; Leofanti, G. Comparison of H₂ Adsorption, O₂ Adsorption, H₂ Titration, and O₂ Titration on Supported Palladium Catalysts. *J. Catal.* **1999**, *181*, 73–79.
- (49) Wang, L.; Yang, F. H.; Yang, R. T.; Miller, M. A. Effect of Surface Oxygen Groups in Carbons on Hydrogen Storage by Spillover. *Ind. Eng. Chem. Res.* **2009**, *48*, 2920–2926.
- (50) Webb, P. A. Introduction to chemical adsorption analytical techniques and their applications to catalysis. *Micromeritics Instrument Corp. Technical Publications*, 2003.
- (51) Amorim, C.; Keane, M. A. Palladium supported on structured and nonstructured carbon: A consideration of Pd particle size and the nature of reactive hydrogen. *J. Colloid Interface Sci.* **2008**, *322*, 196–208.
- (52) Yuan, G.; Keane, M. A. Catalyst deactivation during the liquid phase hydrodechlorination of 2,4-dichlorophenol over supported Pd: influence of the support. *Catal. Today* **2003**, *88*, 27–36.
- (53) Benseradj, F.; Sadi, F.; Chater, M. Hydrogen spillover studies on diluted Rh/Al₂O₃ catalyst. *Appl. Catal. A: Gen.* **2002**, *228*, 135–144.
- (54) Amorim, C.; Wang, X.; Keane, M. A. Application of hydrodechlorination in environmental pollution control: comparison of the performance of supported and unsupported Pd and Ni catalysts. *Chin. J. Catal.* **2011**, *32*, 746–755.

(55) Ouchaib, T.; Moraweck, B.; Massardier, J.; Renouprez, A. Charcoal supported palladium and palladium-chromium catalysts: a comparison in the hydrogenation of dienes with silica supported metals. *Catal. Today* **1990**, *7*, 191–198.